Steel and Composite Structures, *Vol. 35, No. 5 (2020) 659-670*
DOI: https://doi.org/10.12989/scs.2020.35.5.659

The effect of embedding a porous core on the free vibration behavior of laminated composite plates

Babak Safaei*

Department of Mechanical Engineering, Eastern Mediterranean University, G. Magosa, TRNC Mersin 10, Turkey

(*Received March 7, 2020, Revised May 15, 2020, Accepted May 16, 2020*)

Abstract. This paper proposes the use of a porous core between layers of laminated composite plates to examine its effect on the natural frequencies of the resulted porous laminated composite sandwich plate (PLCSP) resting on a two-parameter elastic foundation. Moreover, it has been suggested that the dispersion of porosity has two different functionally graded (FG) patterns which are compared with a uniformly dispersed (UD) profile to find their best vibrational efficiency in the proposed PLCSPs. In FG patterns, two types of dispersions, including symmetric (FG-S) and asymmetric (FG-A) patterns have been considered. To derive the governing Eigen value equation of such structures, the first order shear deformation theory (FSDT) of plates has been employed. Accordingly, a finite element method (FEM) is developed to solve the derived Eigen value equation. Using the mentioned theory and method, the effects of porosity parameters, fiber orientation of laminated composite, geometrical dimensions, boundary conditions and elastic foundation on the natural frequencies of the proposed PLCSPs have been studied. It is observed that embedding porosity in core layer leads to a significant improvement in the natural frequencies of PLCSPs. Moreover, the natural frequencies of PLCSPs with FG porous core are higher than those with UD porous core.

Keywords: porous core; laminated composite; functionally graded; sandwich plate; free vibrations

1. Introduction

Nowadays, porous materials are widely being employed in lightweight structures for decreasing structural weight, damping vibrations, filtering, carrying catalysts, absorbing impact energies and managing thermal responses because of their specific structures and high stiffness to weight ratio (Sciamanna *et al.* 2015). Depends on the demand concerns, different preparation methods have been introduced such as freeze casting (Deville 2008), salt-leaching (Yan *et al.* 2012), synthesis of bio-template (Wu *et al.* 2014), etc. According to the topology of such materials, they can be classified as close or open porous materials. Closed porous materials usually have higher thermal and sonic insulation effects as well as higher stiffness but less permeability (Studart *et al.* 2006). Laminated composite is material another widely used in different industries. This material is extensively utilized in the fabrications of engineering structures such as automotive, civil aircraft and civil infrastructures because laminated composites can address most of the structural concerns related to strength to weight ratio, design flexibility, corrosion resistance and fatigue (Vinson 2001, Zargar *et al.* 2017, Ghanati and Safaei 2019, Xu *et al.* 2019). Besides, sandwich structures basically include a thick low strength core layer to stabilize the structure and two thin stiff face sheets to support the applied loads. Also, the core layer significantly affects the thermo-mechanical behavior and the strength-to-weight ratio of the structure (Safaei *et al.* 2018a, Safaei *et al.* 2019a). Accordingly, it could be expected that the use of porous materials between the plies of laminated composites intensifies the advantages of the traditional laminated composites structures in terms of weight reduction, stiffness improvement, damping vibrations and thermal management (Chen *et al.* 2016, Cong *et al.* 2018). However, the precise design of such porous laminated composite or sandwich structures requires different mechanical analyses.

Due to the significant impacts of composite materials in engineering applications, many researchers have been attracted to research on the mechanical behaviors of structures made of different classes of composites (Safaei *et al.* 2016, Babaei *et al.* 2017, Qin *et al.* 2018, Safaei *et al.* 2019b, Yang *et al.* 2020, Zhang *et al.* 2020). For plates made of laminated composites, Mantari *et al.* (2012) developed an analytical model based on Navier solution and trigonometric theory of plates to study the deflections and stresses of the plates under static loads. For the same plates, Thai *et al.* (2013) established an isogeometric FEM to study vibrations and static responses. To eliminate shear correction factors, they considered FSDT for each layer. Malekzadeh *et al.* (2009) conducted a dynamic study for laminated composite plates subjected to moving loads using layerwise theory. Safaei *et al.* (2018b) investigated an FEM model based on the Galerkin method for analyzing elastic stress field in a platelet reinforced composite subjected to axial load. Setoodeh *et al.* (2009) utilized the theory of 3D elasticity and FEM to evaluate the transient response of laminated composite plates under low velocity impact loads. Tornabene *et al.* (2013) presented a higher order theory to study the vibrational frequencies of doubly-curved panels made of laminated composite materials. Wang

*Corresponding author, Assistant Professor
E-mail: babak.safaei@emu.edu.tr

http://www.techno-press.org/?journal=scs&subpage=8
ISSN: 1229-9367 (Print), 1598-6233 (Online)

(2014) studied the nonlinear wave vibrations of cylindrical shells made of laminated composite materials under radial loads using Galerkin's method. To accomplish this purpose, To eliminate shear locking effect, Yu *et al.* (2016) developed an FSDT based isogeometric analysis on the buckling and vibrational behaviors of laminated composite plates with a random hole. Considering zig-zag effect and utilizing generalized differential quadrature (DQ) method, the static responses of doubly-curved panels made of laminated composite materials located on a nonlinear elastic foundation were presented by Tornabene *et al.* (2017). By developing a Navier's method based on a refined theory of plates, the impact of plate dimensions on the mechanical deflections of laminate composite plates was studied in by Xiaohui *et al.* (2018). Other refined (Sehoul *et al.* 2017) and a higher order plate (Javed *et al.* 2018) theories were also proposed to study the natural frequencies of plates made of laminated composites. The effective material properties of bi-directional functionally graded material were extracted based on Mori-Tanaka, and Hashin–Shtrikman homogenization models proposed numerical analysis for the size-dependent nonlinear bending and postbuckling properties via different homogenization schemes (Sahmani and Safaei 2020). By using the Gurtin–Murdoch theory Li *et al.* (2020) studied nonlinear free vibration behavior of FG composite nanoshells incorporating the influence of modal vibration interaction. In the other work Yi *et al.* (2020) proposed the nonlinear large-amplitude free vibration response of FG porous materials nanoshells by taking into account higher symmetric vibration mode interactions and surface free energy effects. Lateral vibration analysis of simply-supported microbeam under thermal stress is investigated based on both classical and modified couple stress theories (Babaei and Rahmani 2018). Wave propagation was studied in a rotary laminated composite shell with an attached piezoelectric layer using FSDT and considering transverse shear effect in ((Bisheh and Wu, 2018)). Sharma *et al.* (2018) conducted vibroacoustic analysis of laminated composite plates by developing a finite boundary element method. The effect of arbitrary boundary conditions on the natural frequency of laminate composite plates was numerically investigated in by Benhenni *et al.* (2019). Yuan *et al.* (2020) proposed shear buckling behavior of a skew nanoplate made of the FG composite material by using nonlocal theory of elasticity.

Polymers reinforced with different types of nanofillers such as graphene and carbon nanotubes (CNTs) are another popular (nano)composite materials which are being used in engineering structures. Static (Moradi-Dastjerdi *et al.* 2018), vibrations and dynamic behaviors of polymer/CNT (Moradi-Dastjerdi and Payganeh 2017a, 2018, Moradi-Dastjerdi Payganeh *et al.* 2017) as well as polymer/graphene (Moradi-Dastjerdi and Behdinan 2019) cylinders, and polymer/nanoclay plates (Moradi-Dastjerdi *et al.* 2019) were investigated using an axisymmetric meshless method. A unified solution was proposed to study the effect of general boundary conditions on the vibrations and wave propagation responses of polymer/graphene shells in (Qin *et al.* 2019, 2020). The free vibrational responses of plates made of amorphous polyethylene/CNT were examined using DQ method based on different plate theories by Safaei *et al.* (2019c). The impact of CNT agglomeration formation on the nonlinear modal analysis and vibrations of sandwich beams with polymer/CNT was investigated in by Pourasghar and Chen (2019d). The effect of this factor on the thermoelastic dynamic responses of sandwich plates with polymer/CNT faces was also studied (Moradi-Dastjerdi *et al.* 2017; Safaei *et al.* 2019d). Due to the astonishing thermal conductivity of CNTs, the heat transfer (Moradi-Dastjerdi and Payganeh 2017b, Pourasghar and Chen 2019a, Behdinan *et al.* 2020), thermoelastic (Pourasghar and Chen 2019c) and thermoelastic vibrations (Pourasghar *et al.* 2018, Pourasghar and Chen 2019b) of polymer/CNT cylinders, panels and plates have also intensively been analyzed. In addition, the above-mentioned works showed that the use of the concept of ceramic/metal FG materials (Jalali *et al.* 2018, Jalali *et al.* 2018, Fattahi *et al.* 2019a) in the dispersion of nanofillers resulted in significant changes on the thermo-mechanical responses of nanocomposite structures.

Due to the weight advantage of porous materials, their application as single layer structures or as the middle layer of sandwich structures have become an interesting idea to propose lightweight engineering structures. Wang *et al.* (2016) successfully modeled a 3D porosity embedded in volume through an extended FEM simulation. The mechanical responses of metal/ceramic FG plates with FG patterns of embedded porosity dispersions were investigated using a developed polygonal FEM (Nguyen *et al.* 2018). Yang *et al.* (2018) conducted an FSDT based Chebyshev-Ritz solution for the buckling and free vibration Eigenvalue equations of a single FG porous graphene/polymer. For rotary cylindrical shells made of the same porous nanocomposite materials, the backward and forward frequencies of moving waves were calculated by FSDT in (Dong *et al.* 2018). In addition, the static deflection and buckling responses of curved beams made of FG porous metal/graphene mixture were studied using Navier's technique by Polit *et al.* (2019). Zargar *et al.* (2019) employed homotopy approach to study temperature contour in an axisymmetric porous fin. They verified the obtained temperature contour with some numerical results. Xue *et al.* (2019) presented the mode shapes and natural frequencies of circular and rectangular plates with FG embedded voids along the thickness using an expanded isogeometric FEM. The same vibrational analysis was performed for FG porous axisymmetric panels using modified Fourier series (Zhao *et al.* 2019b). Moreover, the vibrations of circular sector plates and annular disks with FG profiles of embedded pores were presented by applying FSDT in by Zhao *et al.* (2019a). Xie *et al.* (2020) investigated the nonlinear resonance behavior of a silicon nanobeam with FG profiles of embedded pore dispersions using the surface theory of elasticity. Nonlinear free vibrations of plates made of an FG mixture of two different piezoceramics with symmetric and asymmetric patterns of porosity dispersions were investigated using an analytical method based on the refined theory of plates (Barati and Zenkour 2018).

Regarding sandwich structures with porous layer(s), Jabbari *et al.* (2013) proposed a circular porous plate located between piezoelectric layers and studied buckling responses of the proposed plate. Askari *et al.* (2018) also presented free vibrational analysis of sandwich plates with the same layer arrangement by applying Mindlin plate theory. Mohammadi *et al.* (2019) attached two piezoelectric faces as sensor and actuator, around FG porous metal cylinders and studied stress and displacement profiles under electro-mechanical loads. Nguyen *et al.* (2019) considered two piezoceramic layers attached onto the faces of an FG porous graphene/polymer with FG patterns of embedded porosity dispersions as sensor and actuator, and developed an FEM model to control the vibrational behavior of the obtained sandwich plates. Also, five-layer sandwich structures with an FG porous core, nanocomposite middle layers and piezoelectric faces have been proposed in literatures. In this regards, the vibrations and buckling loads of such sandwich plates with FG graphene/polymer plates as nanocomposite layers were presented by developing a meshless method in (Moradi-Dastjerdi and Behdinan, 2020b, 2020a). Also, by similar method based on a modified Halpin-Tsai' equation and Reddy's third order theory (TSDT) they proposed the structural damping behavior for piezoelectric sandwich plate (Moradi-Dastjerdi *et al.* 2020c). Setoodeh *et al.* (2019) utilized FG CNT/polymer curved shells as nanocomposite layers and presented natural frequencies of such five-layer curved sandwich shells. Moreover, the buckling responses of polymeric plates located between FG CNT/polymer faces with uniform dispersion of pores embedded along the thickness were presented by applying meshless technique by Safaei *et al.* (2019e). In addition, the thermoelastic static performance of FG porous plates located between FG CNT/polymer faces was studied using a third order of plate theory by Safaei *et al.* (2019f). For rectangular sandwich plates with metal faces and an FG porous graphene/polymer core, a nonlinear natural frequency analysis was conducted in (Li *et al.* 2018).

This paper examines the effect of embedding a porous core between the layers of laminated composite plates on the natural frequencies of the resulted PLCSP. A two-parameter elastic foundation and FG profiles of porosity dispersion have been considered for PLCSP. To study the natural frequency of such structures, Hamilton's principal and FSDT are employed to obtain the governing Eigen value equation. Based on the utilized FSDT, a finite element method is developed to solve the obtained Eigen value equation. The effects of porosity parameters, fiber orientation of laminated composite, geometrical dimension, boundary conditions and elastic foundation on the natural frequencies of the proposed PLCSPs are investigated.

2. Modeling of PLCSP

As shown in Fig. 1, the proposed PLCSP consists of a laminated composite plate which symmetrically integrated a porous core as its middle layer. The fiber orientations α_i (i=1, 2, …, *nl* where *nl* is the number of laminated layers) of composite layers are labeled as [α_1, α_2, …, α_{nl}] starting from the inner to outer layers of each face. In the proposed PLCSP, the length, width, core thickness, faces thickness and total thickness are shown with a, b, h_c, h_f and h, respectively. In addition, the normal and shear parameters of elastic foundation are sown with k_1 and k_2, respectively.

Fig. 2 also illustrates the variations of porosity volume fraction V_p along the thickness of core layer for the three considered porosity patterns. The elasticity modulus E^c, density ρ^c, and Poisson's ratio υ^c of porous layer can be estimated as (Zhao *et al.* 2019b)

$$\text{FG-S:}\quad E^p(z)=\left(1-p_0\cos\left(\frac{\pi z}{h_c}\right)\right)E^m,\qquad \rho^p(z)=\left(1-p_m\cos\left(\frac{\pi z}{h_c}\right)\right)\rho^m \tag{1}$$

$$\text{FG-A:}\quad E^p(z)=\left(1-p_0\cos\left(\frac{\pi z}{4h_c}+\frac{\pi}{4}\right)\right)E^m,\qquad \rho^p(z)=\left(1-p_m\cos\left(\frac{\pi z}{4h_c}+\frac{\pi}{4}\right)\right)\rho^m \tag{2}$$

$$\text{UD:}\quad E^p=\left(\frac{2}{\pi}\sqrt{1-p_0}-\frac{2}{\pi}+1\right)^2E^m,\qquad \rho^p=\left(\frac{2}{\pi}\sqrt{1-p_0}-\frac{2}{\pi}+1\right)\rho^m \tag{3}$$

In all the profiles:

$$\upsilon^p(z)=0.221\beta+\upsilon^m\left(0.342\beta^2-1.21\beta+1\right) \tag{4}$$

where p_0 is porosity parameter, $p_m=1-\sqrt{1-p_0}$, $\beta=1-\rho^p/\rho^m$ and superscript m shows the material properties of perfect ($p_0=0$) core.

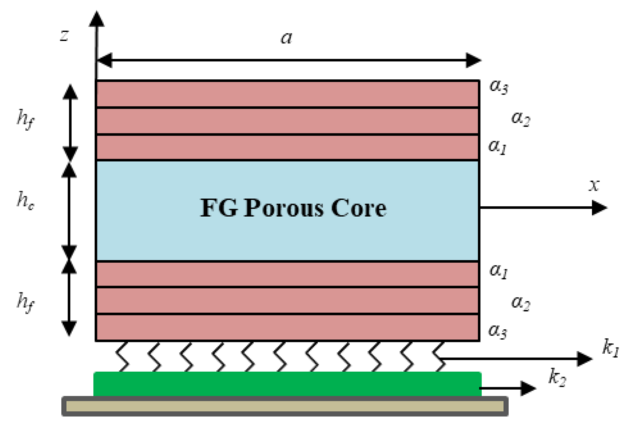

Fig. 1 The proposed PLCSP with a porous core integrated between two laminated composite faces [α_1, α_2, α_3] and rested on an elastic foundation

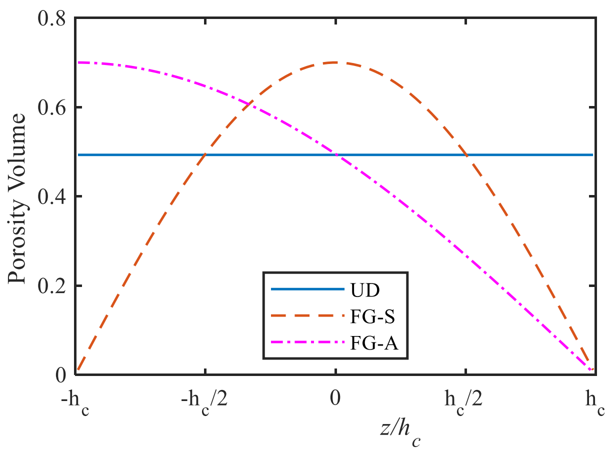

Fig. 2 The distributions of the volume of porosities along the thickness of porous core

3. Governing equations

3.1 Basic equations

For the proposed PLCSP, the equation of energy function U, which includes strain energy, the energy of the two parameter foundation and kinematic energy are determined as follows (Moradi-Dastjerdi *et al.* 2016)

$$U = \frac{1}{2}\int_V \left[\boldsymbol{\varepsilon}_b^T\boldsymbol{\sigma} + \boldsymbol{\gamma}^T\boldsymbol{\tau}\right] - \rho(z)(\dot{u}^2 + \dot{v}^2 + \dot{w}^2)dV \\ \frac{1}{2}\int_A \left[k_1 w^2 + k_2\left[(\partial w/\partial x)^2 + (\partial w/\partial y)^2\right]\right]dA \tag{5}$$

where A and V are the toper (or downer) face area and the total volume of sandwich plate, $\boldsymbol{\sigma}$ and $\boldsymbol{\tau}$ are out-of-plane and in-plane stress vectors, $\boldsymbol{\varepsilon}_b$ and $\boldsymbol{\gamma}$ are out-of-plane and in-plane strain vectors, and u, v and w are the components of displacement field along x, y and z directions, respectively.

As mentioned before, a first order shear deformation theory is utilized to determine displacement field in the proposed PLCSP. This theory has five unknown parameters including u_0, v_0, w_0, φ_x and φ_y which are the displacement components and normal rotations of mid line in sandwich plate. According to the utilized FSDT, the components of displacement field can be defined as (Reddy 2004, Mohammadsalehi *et al.* 2017, Fattahi *et al.* 2019b; Liu *et al.* 2020)

$$\begin{aligned} u &= u_0(x,y) + z\varphi_x(x,y) \\ v &= v_0(x,y) + z\varphi_y(x,y) \\ w &= w_0(x,y) \end{aligned} \tag{6}$$

Based on the defined displacement field, the relation between displacement and strain can be given as (Reddy 2004)

$$\varepsilon_{xx} = \frac{\partial u}{\partial x}, \varepsilon_{yy} = \frac{\partial v}{\partial y}, \gamma_{xy} = \frac{\partial u}{\partial y} + \frac{\partial v}{\partial x} \\ \gamma_{xz} = \frac{\partial u}{\partial z} + \frac{\partial w}{\partial x}, \gamma_{yz} = \frac{\partial v}{\partial z} + \frac{\partial w}{\partial y} \tag{7}$$

By dividing strain components to in-plane and out-of-plane terms, the strain vectors can be written as

$$\boldsymbol{\varepsilon}_b = \begin{Bmatrix} \partial u_0/\partial x \\ \partial v_0/\partial y \\ \partial u_0/\partial y + \partial v_0/\partial x \end{Bmatrix} + z\begin{Bmatrix} \partial \varphi_x/\partial x \\ \partial \varphi_y/\partial y \\ \partial \varphi_x/\partial y + \partial \varphi_y/\partial x \end{Bmatrix} \\ \boldsymbol{\gamma} = \begin{Bmatrix} \varphi_x + \partial w_0/\partial x \\ \varphi_y + \partial w_0/\partial y \end{Bmatrix} \tag{8}$$

These vectors can be rewritten as

$$\boldsymbol{\varepsilon}_b = \{\varepsilon_{xx} \quad \varepsilon_{yy} \quad \gamma_{xy}\}^T = \boldsymbol{\varepsilon}_0 + z\boldsymbol{\varepsilon}_1, \ \boldsymbol{\gamma} = \{\gamma_{xz} \quad \gamma_{yz}\}^T \tag{9}$$

In addition, the constitutive equation, which relates the stress vectors (i.e., in-plane $\boldsymbol{\sigma}$ and out-of-plane $\boldsymbol{\tau}$ stress vectors) to strain vectors, in the proposed PLCSP is defined as (Reddy 2004)

$$\begin{Bmatrix} \sigma_x \\ \sigma_y \\ \sigma_{xy} \end{Bmatrix} = \begin{bmatrix} D_{11} & D_{12} & D_{16} \\ D_{12} & D_{22} & D_{26} \\ D_{26} & D_{26} & D_{66} \end{bmatrix} \begin{Bmatrix} \varepsilon_x \\ \varepsilon_y \\ \gamma_{xy} \end{Bmatrix} \\ \begin{Bmatrix} \tau_{xz} \\ \tau_{yz} \end{Bmatrix} = \frac{5}{6}\begin{bmatrix} D_{55} & D_{45} \\ D_{45} & D_{44} \end{bmatrix} \begin{Bmatrix} \gamma_{xz} \\ \gamma_{yz} \end{Bmatrix} \tag{10}$$

$$\boldsymbol{\sigma} = \mathbf{D_b}\boldsymbol{\varepsilon}_b, \ \boldsymbol{\tau} = \frac{5}{6}\mathbf{D}_s\boldsymbol{\gamma}, \ \mathbf{D} = \begin{bmatrix} \mathbf{D_b} & 0 \\ 0 & \mathbf{D}_s \end{bmatrix} \tag{11}$$

where $\mathbf{D}$ is elastic constant matrix, and the value 5/6 in Eqs. (10) and (11) is came from the use of FSDT as shear correction factor.

The utilized porous core is an isotropic material. In the isotropic materials, D_{ij} are defined as

$$D_{11} = D_{22} = \frac{E^p}{1-(\upsilon^p)^2}, D_{12} = \upsilon^p D_{11}, \\ D_{44} = D_{55} = D_{66} = \frac{E^p}{2(1+\upsilon^p)}, \\ D_{16} = D_{26} = D_{45} = 0 \tag{12}$$

In each layer of laminated composite faces, the matrix of elastic constant is determined by reducing the components related to z direction as

$$D_{ij} = \begin{cases} \bar{Q}_{ij} - (\bar{Q}_{i3}\cdot\bar{Q}_{ij})/Q_{33} & i,j = 1,2,6 \\ \bar{Q}_{ij} & i,j = 4,5 \end{cases} \tag{13}$$

where

$$Q_{11} = E_1\frac{1-\nu_{23}\nu_{32}}{\Delta}, \ Q_{22} = E_2\frac{1-\nu_{13}\nu_{31}}{\Delta} \\ Q_{12} = E_1\frac{\nu_{21}+\nu_{31}\nu_{32}}{\Delta}, Q_{13} = E_3\frac{\nu_{13}+\nu_{12}\nu_{23}}{\Delta} \\ Q_{23} = E_3\frac{\nu_{23}+\nu_{13}\nu_{21}}{\Delta}, Q_{33} = E_3\frac{1-\nu_{12}\nu_{21}}{\Delta} \\ Q_{44} = G_{23}, \ Q_{55} = G_{13}, \ Q_{66} = G_{12} \\ \Delta = \frac{1-\nu_{32}\nu_{23} - \nu_{21}\nu_{12} - \nu_{13}\nu_{31} - 2\nu_{32}\nu_{21}\nu_{13}}{E_1E_2E_3} \tag{14}$$

However, Eq. (14) is valid only for laminated composites with $\alpha = 90^\circ$. For other fiber orientations the components of elastic matrix $\bar{Q}_{ij}$ are determined by the values of $m = \cos\alpha$ and $n = \sin\alpha$ as (Reddy 2004)

$$\begin{aligned}
&\bar{Q}_{11} = m^4 Q_{11} + 2m^2 n^2 \left(Q_{12} + 2Q_{66}\right) + n^4 Q_{22}, \\
&\bar{Q}_{22} = n^4 Q_{11} + 2m^2 n^2 \left(Q_{12} + 2Q_{66}\right) + m^4 Q_{22}, \\
&\bar{Q}_{44} = m^2 Q_{44} + n^2 Q_{55}, \quad \bar{Q}_{55} = m^2 Q_{55} + n^2 Q_{44}, \\
&\bar{Q}_{66} = -m^2 n^2 \left(Q_{11} + Q_{22} - 2Q_{12}\right) + \left(m^4 - n^4\right) Q_{66}, \\
&\bar{Q}_{12} = m^2 n^2 \left(Q_{11} + 4Q_{22} Q_{66}\right) + \left(m^4 + n^4\right) Q_{12}, \\
&\bar{Q}_{13} = m^2 Q_{13} + n^2 Q_{23}, \quad \bar{Q}_{23} = n^2 Q_{13} + m^2 Q_{23}, \\
&\bar{Q}_{36} = \left(Q_{32} - Q_{31}\right) mn, \quad \bar{Q}_{45} = \left(Q_{45} - Q_{55}\right) mn, \\
&\bar{Q}_{16} = -mn\left[n^2 Q_{11} - m^2 Q_{22} - \left(m^2 - n^2\right)\left(Q_{12} + 2Q_{66}\right)\right] \\
&\bar{Q}_{26} = -mn\left[m^2 Q_{11} - n^2 Q_{22} - \left(m^2 - n^2\right)\left(Q_{12} + 2Q_{66}\right)\right]
\end{aligned} \tag{15}$$

3.2 FEM formulations

After generating elements, finite element methods approximate the real values of domain at some specific points called nodes. In this work, the desired domain is displacement field, and rectangular elements with only four nodes have been employed. The relation between the displacement field $\mathbf{u}$ and that approximated by FEM u_i is determined as

$$\mathbf{u} = \sum_{i=1}^{n} N_i u_i \tag{16}$$

where n is the total number of nodes and N_i is bilinear shape functions. The use of FSDT dictates five unknowns or degrees of freedom to each node. So, the vector of approximated nodal values is determined as (Moradi-Dastjerdi *et al.* 2016)

$$u_i = \left[u_{0i}, v_{0i}, w_{0i}, \varphi_{xi}, \varphi_{yi}\right]^T \tag{17}$$

Introducing Eq. (16) in Eq. (7) results in the FEM forms of strain vectors

$$\boldsymbol{\varepsilon}_b = \left\{\mathbf{B}_m + z\,\mathbf{B}_b\right\}\mathbf{u} \quad , \quad \boldsymbol{\gamma} = \mathbf{B}_s\,\mathbf{u} \tag{18}$$

where

$$\begin{aligned}
\mathbf{B}_s &= \begin{bmatrix} 0 & 0 & N_{i,x} & N_i & 0 \\ 0 & 0 & N_{i,y} & 0 & N_i \end{bmatrix} \\
\mathbf{B}_m &= \begin{bmatrix} N_{i,x} & 0 & 0 & 0 & 0 \\ 0 & N_{i,y} & 0 & 0 & 0 \\ N_{i,y} & N_{i,x} & 0 & 0 & 0 \end{bmatrix} \\
\mathbf{B}_b &= \begin{bmatrix} 0 & 0 & 0 & N_{i,x} & 0 \\ 0 & 0 & 0 & 0 & N_{i,y} \\ 0 & 0 & 0 & N_{i,y} & N_{i,x} \end{bmatrix}
\end{aligned} \tag{19}$$

Introducing the FEM definitions of displacement, strain and stress vectors in the total energy function (Eq. (15)) results in

$$\begin{aligned}
U &= \frac{1}{2}\int_{\Omega} \mathbf{u}^T \left\{\begin{matrix} \mathbf{B}_m^T \mathbf{A} \mathbf{B}_m + \mathbf{B}_m^T \bar{\mathbf{B}} \mathbf{B}_b + \mathbf{B}_b^T \bar{\mathbf{B}} \mathbf{B}_m \\ + \mathbf{B}_b^T \mathbf{D} \mathbf{B}_b + \mathbf{B}_s^T \mathbf{A}_s \mathbf{B}_s \end{matrix}\right\} \mathbf{u}\, dA \\
&+ \frac{1}{2}\int_{\Omega} \mathbf{u}^T \left\{\mathbf{B}_n^T k_1 \mathbf{B}_n + \mathbf{B}_{s2}^T k_2 \mathbf{B}_{s2}\right\} \mathbf{u}\, dA \\
&- \frac{1}{2}\int_{A} \ddot{\mathbf{u}}^T \int_{z} \left[\mathbf{G}_i^T \bar{\mathbf{M}} \mathbf{G}_j\right] \ddot{\mathbf{u}} dA
\end{aligned} \tag{20}$$

where

$$(\mathbf{A}, \bar{\mathbf{B}}, \mathbf{D}) = \int_{-h/2}^{h/2} \mathbf{D}_b (1, z, z^2) dz, \mathbf{A}_s = \frac{5}{6}\int_{-h/2}^{h/2} \mathbf{D}_s dz \tag{21}$$

$$\begin{aligned}
\mathbf{B}_n &= \begin{bmatrix} 0 & 0 & N_i & 0 & 0 \end{bmatrix}, \\
\mathbf{B}_{s2} &= \begin{bmatrix} 0 & 0 & N_{i,x} & 0 & 0 \\ 0 & 0 & N_{i,y} & 0 & 0 \end{bmatrix}
\end{aligned} \tag{22}$$

$$\mathbf{G}_i = \begin{bmatrix} \varphi_i & 0 & 0 & 0 & 0 \\ 0 & \varphi_i & 0 & 0 & 0 \\ 0 & 0 & \varphi_i & 0 & 0 \\ 0 & 0 & 0 & \varphi_i & 0 \\ 0 & 0 & 0 & 0 & \varphi_i \end{bmatrix} \tag{23}$$

$$\bar{\mathbf{M}} = \begin{bmatrix} I_0 & 0 & 0 & I_1 & 0 \\ 0 & I_0 & 0 & 0 & I_1 \\ 0 & 0 & I_0 & 0 & 0 \\ I_1 & 0 & 0 & I_2 & 0 \\ 0 & I_1 & 0 & 0 & I_2 \end{bmatrix} \tag{24}$$

In addition, I_0, I_1 and I_2 are the coefficient of inertia which are defined as

$$(I_0, I_1, I_2) = \int_{-h/2}^{h/2} \rho(z)(1, z, z^2) dz \tag{25}$$

The use of Hamilton's principle in Eq. (20) results in the following Eigen value governing equation for the proposed PLCSP

$$\mathbf{M}\ddot{\mathbf{u}} + \mathbf{K}\mathbf{u} = 0 \tag{26}$$

where $\mathbf{M}$ and $\mathbf{K}$ are the global stiffness and mass matrices which are determined as

$$\mathbf{M} = \int_{A} \mathbf{G}_i^T \bar{\mathbf{M}} \mathbf{G}_j dA \tag{27}$$

$$\begin{aligned}
\mathbf{K} &= \int_{\Omega} \left\{\begin{matrix} \mathbf{B}_m^T \mathbf{A} \mathbf{B}_m + \mathbf{B}_m^T \bar{\mathbf{B}} \mathbf{B}_b + \mathbf{B}_b^T \bar{\mathbf{B}} \mathbf{B}_m \\ + \mathbf{B}_b^T \mathbf{D} \mathbf{B}_b + \mathbf{B}_s^T \mathbf{A}_s \mathbf{B}_s \end{matrix}\right\} d\Omega \\
&+ \int_{\Omega} \left\{\mathbf{B}_n^T k_1 \mathbf{B}_n + \mathbf{B}_{s2}^T k_2 \mathbf{B}_{s2}\right\} d\Omega
\end{aligned} \tag{28}$$

4. Results and discussions

In this section, first, the reliability of the developed FEM is established and then, the free vibration behavior of the proposed PLCSP is studied. It is assumed that the laminate composite faces and the porous core of PLCSPs are made of graphite–epoxy (Gr/Ep) and neat epoxy, respectively. Moreover, in the following simulations, clamped (CCCC) square PLCSPs with four-layer laminated composite faces [0, 90, 0, 90], h_c/a = 0.01, h_f/h_c = 0.2, and $K_1 = K_2 = 0$ (without elastic foundation) have been considered, unless otherwise clearly stated. In addition, the following material properties have been considered (Talebitooti *et al.* 2016):

Epoxy: ρ=1150 Kg/m^3, E=4.5 GPa, υ=0.4

Gr/Ep: ρ=1578 Kg/m^3, E_{11}=132.38 GPa, $E_{12}=E_{13}$=10.756 GPa, G_{23}=3.606e9 GPa, $G_{12}=G_{13}$=5.6537 GPa, υ_{23}=0.49, $\upsilon_{12}=\upsilon_{13}$=0.24

The following normalized parameters are also utilized for natural frequency Ω and foundation coefficients K_1, K_2 in this section

$$\Omega = \omega H_0 \sqrt{\rho^p / E^p}$$
$$K_1 = k_1 a^4 / D\,, \quad K_2 = k_2 a^4 / D \tag{29}$$

where

$$D = E^p h^3 / 12\left(1-\left(\upsilon^p\right)^2\right) \quad \text{and} \quad H_0 = 0.1\,m \tag{30}$$

In this paper, sandwich plates with different types of boundary conditions on their edges including clamped (C), simply supported (S) and free (F) edges have been considered. To implement such boundary conditions, the following descriptions have been utilized:

C edges: "$u = v = w = \varphi_x = \varphi_y = 0$"

S edges: "$u = w = \varphi_x = 0$ at $y = 0$ or a" and "$v = w = \varphi_y = 0$ at x=0 or b"

4.1 Validation of models

In order to examine the accuracy of the developed method, square simply supported isotropic plates with E=380 GPa, ρ=3800 Kg/m^3, υ=0.3 and different thicknesses have been considered and their natural frequencies obtained from our developed FEM are compared with those available in literatures as summarized in Table 1. The comparison of the nondimensional fundamental frequency of plates shows that the developed FEM has a very good agreement with the reported results, especially for thin and moderately thick plates. This is because our formulation is based on FSDT formulation; however, higher order theories have been employed in by Baferani *et al.* (2011). This comparison also reveals that the formulation developed in this paper is computationally efficient because it is based on FSDT with only five unknowns and employs bilinear rectangular element which do not impose huge computational costs.

In addition, the convergence of the developed FEM in the calculation of the fundamental natural frequency of the proposed PLCSP with a porous core is also examined. Fig. 3 shows the variation of Ω as a function of node number along each direction N (x or y) when the porosity state is FG-S and p_0=0.9. This figure shows that the addition of node number after the use of 15×15 nodes does not significantly change the value of Ω which shows the convergence of the developed FEM.

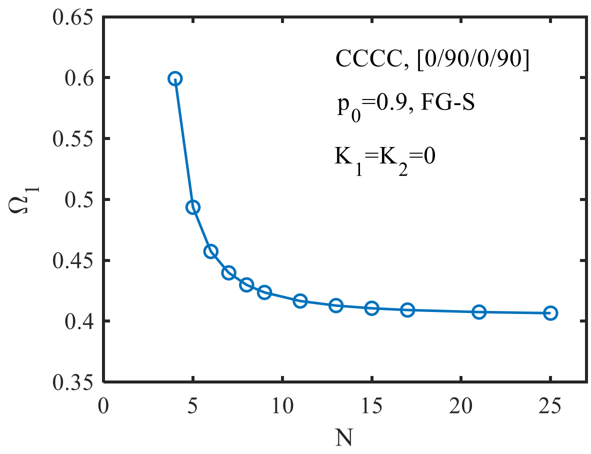

Fig. 3 Nondimensional fundamental natural frequency of PLCSP as a function of node number

Table1 The nondimensional fundamental natural frequency of square simply supported

h/a	**Method**	Ω
0.05	Baferani *et al.* (2011)	0.0291
	Thai and Choi (2011)	0.0291
	Moradi-Dastjerdi *et al.* (2016)	0.0291
	Present	**0.0292**
0.1	Baferani *et al.* (2011)	0.1134
	Thai and Choi (2011)	0.1135
	Moradi-Dastjerdi *et al.* (2016)	0.1135
	Present	**0.1136**
0.2	Baferani *et al.* (2011)	0.4154
	Thai and Choi (2011)	0.4154
	Moradi-Dastjerdi *et al.* (2016)	0.4167
	Present	**0.4159**

4.2 Free vibration of PLCSPs

One of the main parameters in structures made of laminated composite materials is their fiber orientation or stacking sequence. For the proposed PLCSP with the porosity state of FG-S and p_0=0.9, Table 2 shows the effect of stacking sequence in laminate composite faces on the first four natural frequencies. Among the four considered stacking sequence, it is observed that [0, 90, 0, 90] offers the highest values of natural frequencies while, PLCSP with [45, -45, 45, -45] faces has the lowest values of natural frequencies.

Fig. 4 illustrates the first four mode shapes of vibrations for PLCSPs with [0, 90, 0, 90] and [45, -45, 45, -45]. This figure confirms that stacking sequence has a significant effect on the mode shapes of vibrations.

Another parameter in such structures is the number of layers nl. The effect of this parameter on the fundamental natural frequency of PLCSPs with porous (FG-S and p_0=0.2) and perfect cores is shown in Fig. 5. This figure shows that the increase of nl has an insignificant effect on natural frequency such that PLCSPs with nl >2 have almost the same Ω_1. However, embedding porosity in core layer results in higher natural frequencies.

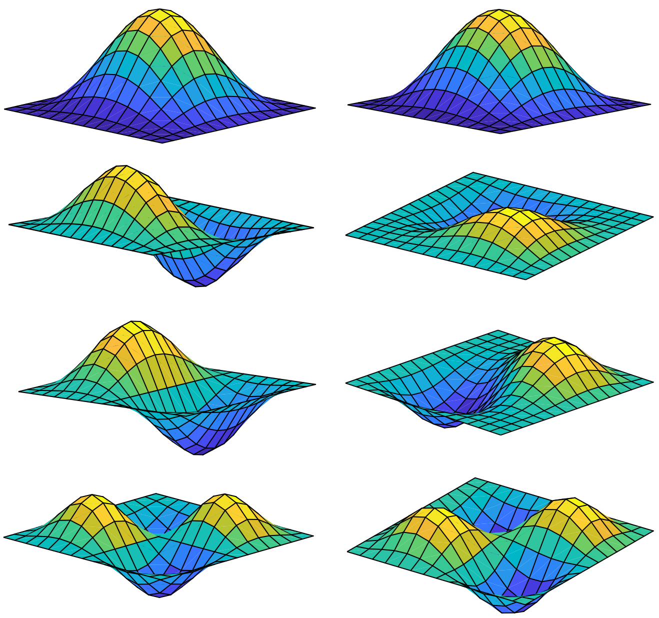

(a) [0, 90, 0, 90] (b) [45, -45, 45, -45]

Fig. 4 First four mode shapes of vibration in PLCSP with (a) [0, 90, 0, 90] (b) [45, -45, 45, -45] faces

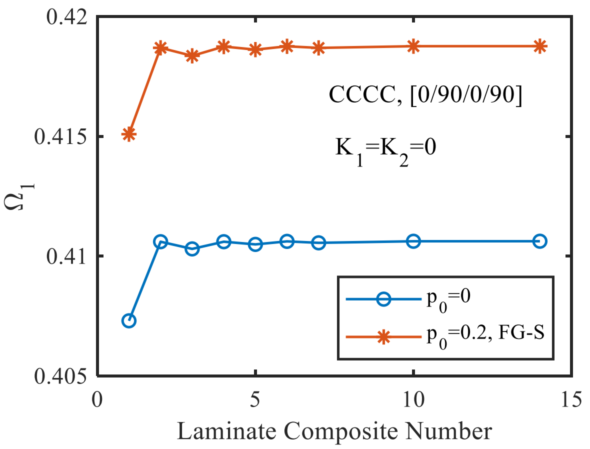

Fig. 5 The variation of fundamental Ω versus the number of laminated layers in PLCSP with porous (FG-S and p_0=0.2) and perfect core

Table 2 The first four Ω for PLCSPs with FG-S, p_0=0.9 and different stacking sequences

[α_1, α_2, α_3, α_4]	Ω_1	Ω_2	Ω_3	Ω_4
[45, -45, 45, -45]	0.4613	0.9284	0.9441	1.4574
[0, 30, 60, 90]	0.4648	0.8936	1.0270	1.3308
[0, 45, 90, -45]	0.4702	0.9416	0.9922	1.4180
[0, 90, 0, 90]	0.4784	0.9734	1.0203	1.3609

The effect of porosity state, including the volume of porosity and the profile of their dispersion, is also investigated in Fig. 6. This figure shows the Ω_1 of such PLCSPs with two different values of core thickness; i.e.,

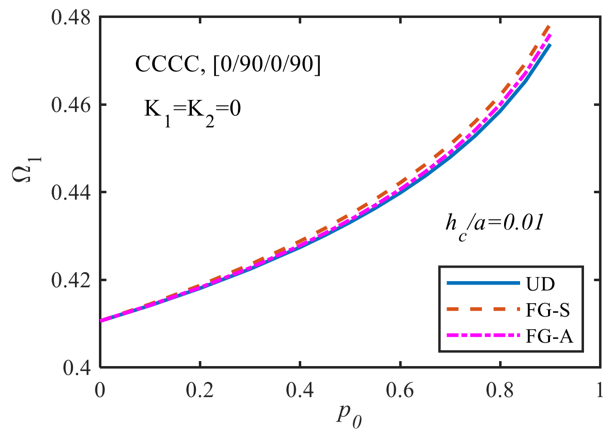

(a)

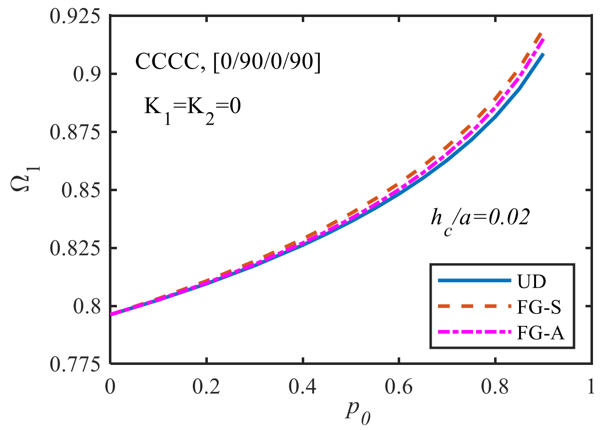

(b)

Fig. 6 The variation of fundamental Ω versus porosity parameter in PLCSPs with (a) h_c/a = 0.01 (b) h_c/a = 0.02

h_c/a = 0.01 and 0.02. The figures show that the increase of p_0, which implies the increase of porosity volume, leads to the enhancement of natural frequency. The reason is the structural weight is remarkably reduced by embedding higher voids in the thickest layer of PLCSP. In addition, it is observed that the dispersion pattern of voids does not have a significant impact on the natural frequency of PLCSP although FG-S type sandwich plates have higher Ω_1. The comparison between Figs. 6(a) and 6(b) shows that the increase of core thickness significantly enhances the natural frequency of the PLCSP.

The effects of aspect ratio (b/a) and the length of sides (a/h_c) on the natural frequency of PLCSPs are shown in Figs. 7 and 8, respectively. These figures show fundamental Ω_1 for PLCSPs with porous and perfect cores and two values of h_f/h_c=0.1 and 0.2. Fig. 7 shows that, in all cases, a small increase of the aspect ratio of plates from b/a=1 dramatically reduces the natural frequencies of PLCSPs. The rate of this reduction becomes insignificant for b/a>4. Fig. 8 also shows that the increase of the length of sides continuously reduces the natural frequency of PLCSPs.

Moreover, the significant effect of the thickness of composite faces are evident in both perfect and porous sandwich plates such that the use of thicker composite faces offers much higher natural frequencies. The comparison between the results of PLCSPs with porous and perfect cores (Figs. 7(a) and 7(b) and Figs. 8(a) and 8(b)) shows that the use of porous core results in higher PLCSPs with higher natural frequencies.

Finally, the effect the remaining parameters of the PLCSP, i.e., boundary conditions (F, C and S imply free, clamped and simply supported edges, respectively) and the coefficients of elastic foundation, on the natural frequencies of the proposed PLCSPs are studied. Table 3 shows Ω_1 for PLCSP with FG-S type core. As expected, PLCSPs with four clamped edges have the highest values of natural frequency and by changing clamped edges to simply supported and then free ones, the natural frequency of the plate is decreased due to losing some constrains in each edge such that the lowest natural frequencies are observed in sandwich SFSF plates. Moreover, the enhancement of natural frequency is observed due to the use of elastic foundation such that the shear effect of foundation K_2 has stronger impact on the natural frequency of PLCSPs than the normal one K_1.

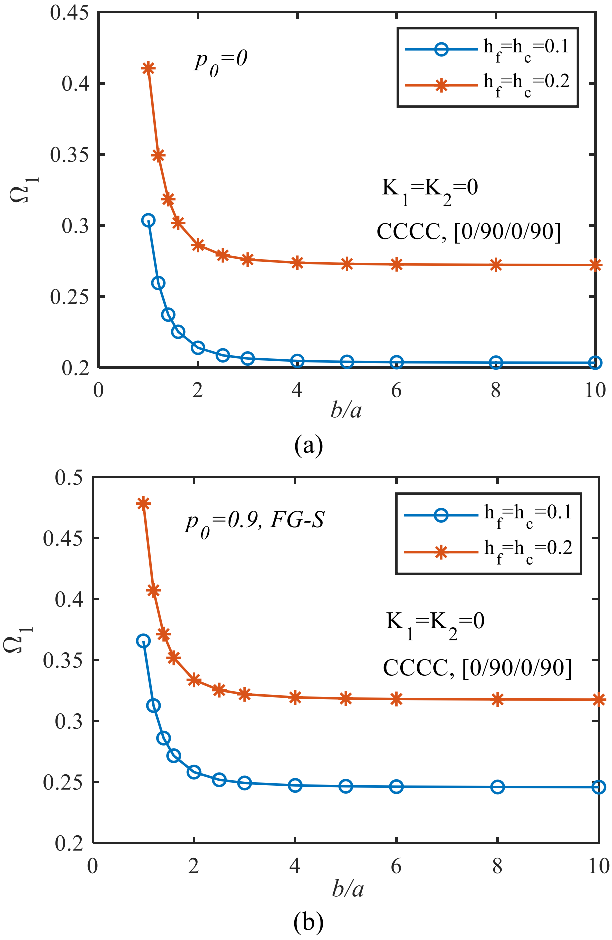

Fig. 7 The variation of fundamental Ω versus the aspect ratio of plate in PLCSPs with (a) perfect and (b) porous cores

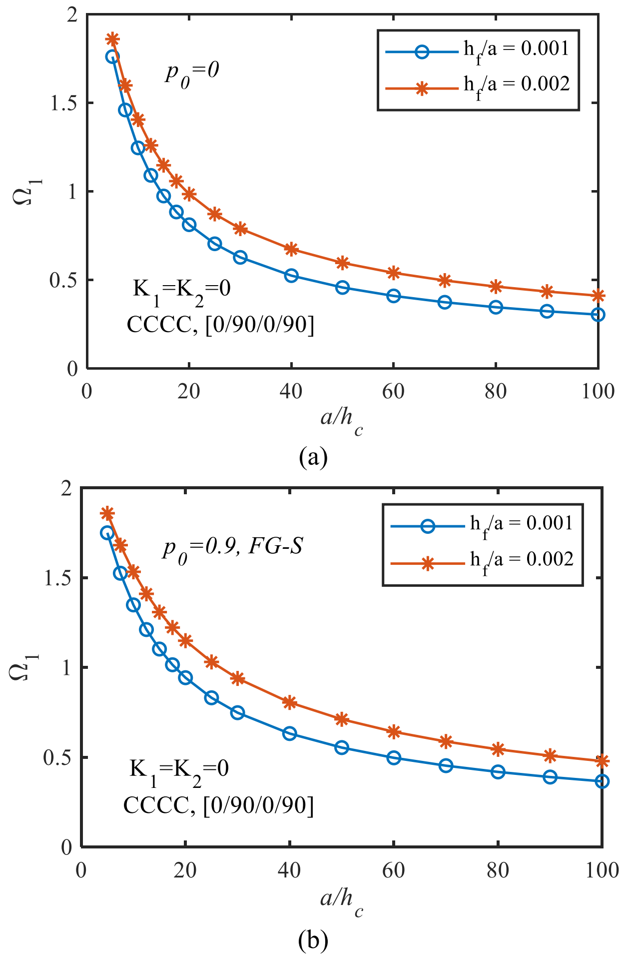

Fig. 8 The variation of fundamental Ω versus a/h_c of for PLCSPs with (a) perfect and (b) porous cores

Table 3 Fundamental Ω for PLCSPs with FG-S type core

B.C.	K_1,K_2	p_0=0	p_0=0.5	p_0=0.9
CCCC	**(0,0)**	0.4106	0.4350	0.4784
	(500,0)	0.4144	0.4391	0.4830
	(0,50)	0.4199	0.4449	0.4895
CSCS	**(0,0)**	0.3273	0.3468	0.3815
	(500,0)	0.3322	0.3520	0.3872
	(0,50)	0.3379	0.3581	0.3941
CFCF	**(0,0)**	0.2905	0.3081	0.3392
	(500,0)	0.2959	0.3139	0.3459
	(0,50)	0.2972	0.3152	0.3471
SSSS	**(0,0)**	0.1940	0.2054	0.2259
	(500,0)	0.2020	0.2140	0.2355
	(0,50)	0.2096	0.2222	0.2446
SFSF	**(0,0)**	0.1279	0.1358	0.1498
	(500,0)	0.1398	0.1486	0.1639
	(0,50)	0.1398	0.1485	0.1638

5. Conclusions

This paper examined the effect of embedding a porous core between the layers of laminated composite plates on the natural frequencies of a new PLCSP resting on elastic foundations. The governing Eigen value equation of such structures was obtained using Hamilton's principal and FSDT. To solve the obtained equation, a finite element method was developed for this particular structure. The significant results of this study are as follows:

- The use of laminated faces with stacking sequence of [0, 90, 0, 90] results in PLCSPs with the highest natural frequencies.
- The addition of layers in laminated composite faces after *nl* >2 has an insignificant effect on the natural frequency of PLCSPs.
- Embedding a core between the layers of laminated composite plates enhances the natural frequencies of the resulted structures.
- In addition, embedding porosity in core layer leads to a significant improvement in the natural frequencies of PLCSPs.
- The natural frequencies of PLCSPs with FG porous cores are higher than those with UD porous cores.
- A small increase in the aspect ratio of plates from b/a=1 dramatically reduces the natural frequencies of PLCSPs.
- The effect of face thickness on the natural frequency of PLCSPs are stronger than core thickness.

References

Askari, M., Saidi, A.R. and Rezaei, A.S. (2018), "An investigation over the effect of piezoelectricity and porosity distribution on natural frequencies of porous smart plates", *J. Sandw. Struct. Mater.*, doi: 10.1177/1099636218791092.

Babaei, A., Noorani, M.R.S. and Ghanbari, A. (2017), "Temperature-dependent free vibration analysis of functionally graded micro-beams based on the modified couple stress theory", *Microsyst. Technol.*, **23**(10), 4599-4610. doi: 10.1007/s00542-017-3285-0.

Babaei, A. and Rahmani, A. (2018), "On dynamic-vibration analysis of temperature-dependent Timoshenko microbeam possessing mutable nonclassical length scale parameter", *Mech. Adv. Mater. Struct.*, doi: 10.1080/15376494.2018.1516252.

Baferani, A.H., Saidi, A.R. and Ehteshami, H. (2011), "Accurate solution for free vibration analysis of functionally graded thick rectangular plates resting on elastic foundation", *Compos. Struct.*, **93**(7), 1842-1853. doi: https://doi.org/10.1016/j.compstruct.2011.01.020.

Barati, M.R. and Zenkour, A.M. (2018), "Electro-thermoelastic vibration of plates made of porous functionally graded piezoelectric materials under various boundary conditions", *J. Vib. Control*, **24**(10), 1910-1926. doi: 10.1177/1077546316672788.

Behdinan, K., Moradi-Dastjerdi, R., Safaei, B., Qin, Z., Chu, F. and Hui, D. (2020), "Graphene and CNT impact on heat transfer response of nanocomposite cylinders", *Nanotechnol. Rev.*, **9**, 41-52. Available at: https://doi.org/10.1515/ntrev-2020-0004.

Benhenni, M.A., Daouadji, T.H., Abbès, B., Abbès, F., Li, Y. and Adim, B. (2019), "Numerical analysis for free vibration of hybrid laminated composite plates for different boundary conditions", *Struct. Eng. Mech.*, **70**(5), 535-549. doi: 10.12989/sem.2019.70.5.535.

Bisheh, H.K. and Wu, N. (2018), "Wave propagation characteristics in a piezoelectric coupled laminated composite cylindrical shell by considering transverse shear effects and rotary inertia", *Compos. Struct.*, **191**, 123-144. doi: 10.1016/j.compstruct.2018.02.010.

Chen, D., Kitipornchai, S. and Yang, J. (2016), "Nonlinear free vibration of shear deformable sandwich beam with a functionally graded porous core", *Thin-Wall. Struct.*, **107**, 39-48. doi: 10.1016/j.tws.2016.05.025.

Cong, P.H., Chien, T.M., Khoa, N.D. and Duc, N.D. (2018), "Nonlinear thermomechanical buckling and post-buckling response of porous FGM plates using Reddy's HSDT", *Aerosp. Sci. Technol.*, **77**, 419-428. doi: 10.1016/j.ast.2018.03.020.

Deville, S. (2008), "Freeze-casting of porous ceramics: A review of current achievements and issues", *Adv. Eng. Mater.*, 155-169. doi: 10.1002/adem.200700270.

Dong, Y.H., Li, Y.H., Chen, D. and Yang, J. (2018), "Vibration characteristics of functionally graded graphene reinforced porous nanocomposite cylindrical shells with spinning motion", *Compos. Part B Eng.*, **145**, 1-13. doi: 10.1016/j.compositesb.2018.03.009.

Fattahi, A.M., Safaei, B. and Moaddab, E. (2019a), "The application of nonlocal elasticity to determine vibrational behavior of FG nanoplates", *Steel Compos. Struct.*, **32**(2), 281-292. https://doi.org/10.12989/scs.2019.32.2.281.

Fattahi, A.M., Safaei, B. and Ahmed, N.A. (2019b), "A comparison for the non-classical plate model based on axial buckling of single-layered graphene sheets", *Eur. Phys. J. Plus*, **134**(11), 555. doi: 10.1140/epjp/i2019-12912-7.

Ghanati, P. and Safaei, B. (2019), "Elastic buckling analysis of polygonal thin sheets under compression", *Indian J. Phys.*, **93**(1), 47-52. doi: 10.1007/s12648-018-1254-9.

Jabbari, M., Joubaneh, E.F., Khorshidvand, A.R. and Eslami, M.R. (2013), "Buckling analysis of porous circular plate with piezoelectric actuator layers under uniform radial compression", *Int. J. Mech. Sci.*, **70**, 50–56. doi: 10.1016/j.ijmecsci.2013.01.031.

Jalali, M.H., Shahriari, B., Zargar, O., Baghani, M. and Baniassadi, M. (2018), "Free vibration analysis of rotating functionally graded annular disc of variable thickness using generalized differential quadrature method", *Sci. Iran.*, **25**(2), 728-740. doi: 10.24200/SCI.2017.4325.

Jalali, M.H., Zargar, O. and Baghani, M. (2018), "Size-dependent vibration analysis of FG microbeams in thermal environment based on modified couple stress theory", *Iran. J. Sci. Technol. Trans. Mech. Eng.* doi: 10.1007/s40997-018-0193-6.

Javed, S., Viswanathan, K.K., Izyan, M.D.N., Aziz, Z.A. and Lee, J.H. (2018), "Free vibration of cross-ply laminated plates based on higher-order shear deformation theory", *Steel Compos. Struct.*, **26**(4), 473-484. https://doi.org/10.12989/scs.2018.26.4.473.

Li, Q., Wu, D., Chen, X., Liu, L., Yu, Y. and Gao, W. (2018), "Nonlinear vibration and dynamic buckling analyses of sandwich functionally graded porous plate with graphene platelet reinforcement resting on Winkler–Pasternak elastic foundation", *Int. J. Mech. Sci.*, **148**, 596-610. doi: 10.1016/J.IJMECSCI.2018.09.020.

Li, Q., Xie, B., Sahmani, S. and Safaei, B. (2020), "Surface stress effect on the nonlinear free vibrations of functionally graded composite nanoshells in the presence of modal interaction", *J. Brazilian Soc. Mech. Sci. Eng.*, **42**(5), 237. doi: 10.1007/s40430-020-02317-2.

Liu, T., Wang, A., Wang, Q. and Qin, B. (2020), "Wave based method for free vibration characteristics of functionally graded cylindrical shells with arbitrary boundary conditions", *Thin-Wall. Struct.*, **148**. doi: 10.1016/j.tws.2019.106580.

Malekzadeh, P., Fiouz, A.R. and Razi, H. (2009), "Three-dimensional dynamic analysis of laminated composite plates subjected to moving load", *Compos. Struct.*, **90**(2), 105-114. doi: 10.1016/j.compstruct.2009.02.008.

Mantari, J.L., Oktem, A.S. and Guedes Soares, C. (2012), "A new trigonometric shear deformation theory for isotropic, laminated composite and sandwich plates", *Int. J. Solids Struct.*, **49**(1), 43-53. doi: 10.1016/j.ijsolstr.2011.09.008.

Mohammadi, M., Bamdad, M., Alambeigi, K., Dimitri, R. and Tornabene, F. (2019), "Electro-elastic response of cylindrical sandwich pressure vessels with porous core and piezoelectric face-sheets", *Compos. Struct.*, **225**, 111119. doi: 10.1016/J.COMPSTRUCT.2019.111119.

Mohammadsalehi, M., Zargar, O. and Baghani, M. (2017), "Study of non-uniform viscoelastic nanoplates vibration based on nonlocal first-order shear deformation theory", *Meccanica*, **52**, 1063–1077. doi: 10.1007/s11012-016-0432-0.

Moradi-Dastjerdi, R., Payganeh, G., Rajabizadeh Mirakabad, S. and Jafari Mofrad Taheri, M. (2016), "Static and free vibration analyses of functionally graded nano- composite plates reinforced by wavy carbon nanotubes resting on a pasternak elastic foundation", *Mech. Adv. Compos. Struct.*, **3**, 123-135. doi: 10.22075/macs.2016.474.

Moradi-Dastjerdi, R. and Behdinan, K. (2019), "Thermoelastic static and vibrational behaviors of nanocomposite thick cylinders reinforced with graphene", *Steel Compos. Struct.*, **31**(5), 529-539. https://doi.org/10.12989/scs.2019.31.5.529.

Moradi-Dastjerdi, R. and Behdinan, K. (2020a), "Stability analysis of multifunctional smart sandwich plates with graphene nanocomposite and porous layers", *Int. J. Mech. Sci.*, **167**, 105283. doi: 10.1016/j.ijmecsci.2019.105283.

Moradi-Dastjerdi, R. and Behdinan, K. (2020b), "Temperature effect on free vibration response of a smart multifunctional sandwich plate", *J. Sandw. Struct. Mater.*, DOI: 10.1177/1099636220908707. Available at: https://doi.org/10.1177/1099636220908707.

Moradi-Dastjerdi, R., Malek-Mohammadi, H. and Momeni-Khabisi, H. (2017), "Free vibration analysis of nanocomposite sandwich plates reinforced with CNT aggregates", *ZAMM - J. Appl. Math. Mech. / Zeitschrift fur Angew. Math. und Mech.*, **97**(11), 1418–1435. doi: 10.1002/zamm.201600209.

Moradi-Dastjerdi, R., Meguid, S.A. and Rashahmadi, S. (2019), "Electro-dynamic analysis of smart nanoclay-reinforced plates with integrated piezoelectric layers", *Appl. Math. Model.*, **75**, 267-278. doi: 10.1016/j.apm.2019.05.033.

Moradi-Dastjerdi, R. and Payganeh, G. (2017a), "Thermoelastic dynamic analysis of wavy carbon nanotube reinforced cylinders under thermal loads", *Steel Compos. Struct.*, **25**(3), 315-326. https://doi.org/10.12989/scs.2017.25.3.315.

Moradi-Dastjerdi, R. and Payganeh, G. (2017b), "Transient heat transfer analysis of functionally graded CNT reinforced cylinders with various boundary conditions", *Steel Compos. Struct.*, **24**(3), 359-367. https://doi.org/10.12989/scs.2017.24.3.359.

Moradi-Dastjerdi, R. and Payganeh, G. (2018), "Thermoelastic Vibration Analysis of Functionally Graded Wavy Carbon Nanotube-Reinforced Cylinders", *Polym. Compos.*, **39**(S2), E826-E834. doi: 10.1002/pc.24278.

Moradi-Dastjerdi, R., Payganeh, G. and Tajdari, M. (2017), "Resonance in Functionally Graded Nanocomposite Cylinders Reinforced by Wavy Carbon Nanotube", *Polym. Compos.*, **38**, E542–E552. doi: 10.1002/pc.24045.

Moradi-Dastjerdi, R., Payganeh, G. and Tajdari, M. (2018), "Thermoelastic Analysis of Functionally Graded Cylinders Reinforced by Wavy CNT Using a Mesh-Free Method", *Polym. Compos.*, **39**(7), 2190-2201. doi: 10.1002/pc.24183.

Moradi-Dastjerdi, R., Radhi, A. and Behdinan, K. (2020c), "Damped dynamic behavior of an advanced piezoelectric sandwich plate", *Compos. Struct.*, 112243. doi: 10.1016/j.compstruct.2020.112243.

Nguyen, N.V., Lee, J. and Nguyen-Xuan, H. (2019), "Active vibration control of GPLs-reinforced FG metal foam plates with piezoelectric sensor and actuator layers", *Compos. Part B Eng.*, **172**, 769-784. doi: 10.1016/J.COMPOSITESB.2019.05.060.

Nguyen, N.V, Nguyen, H.X., Lee, S. and Nguyen-xuan, H. (2018), "Geometrically nonlinear polygonal finite element analysis of functionally graded porous plates", *Adv. Eng. Softw.*, **126**, 110-126. doi: 10.1016/j.advengsoft.2018.11.005.

Polit, O., Anant, C., Anirudh, B. and Ganapathi, M. (2019), "Functionally graded graphene reinforced porous nanocomposite curved beams : Bending and elastic stability using a higher-order model with thickness stretch effect", *Compos. Part B*, **166**, 310-327. doi: 10.1016/j.compositesb.2018.11.074.

Pourasghar, A., Moradi-Dastjerdi, R., Yas, M.H., Ghorbanpour Arani, A. and Kamarian, S. (2018), "Three-dimensional analysis of carbon nanotube- reinforced cylindrical shells with temperature- dependent properties under thermal environment", *Polym. Compos.*, **39**(4), 1161-1171. doi: 10.1002/pc.24046.

Pourasghar, A. and Chen, Z. (2019a), "Dual-phase-lag heat conduction in FG carbon nanotube reinforced polymer composites", *Phys. B Condens. Matter*, **564**, 147-156. doi: 10.1016/j.physb.2019.03.038.

Pourasghar, A. and Chen, Z. (2019b), "Effect of hyperbolic heat conduction on the linear and nonlinear vibration of CNT reinforced size-dependent functionally graded microbeams", *Int. J. Eng. Sci.*, **137**, 57-72. doi: 10.1016/j.ijengsci.2019.02.002.

Pourasghar, A. and Chen, Z. (2019c) "Hyperbolic heat conduction and thermoelastic solution of functionally graded CNT reinforced cylindrical panel subjected to heat pulse", *Int. J. Solids Struct.*, **163**, 117–129. Available at: https://doi.org/10.1016/j.ijsolstr.2018.12.030.

Pourasghar, A. and Chen, Z. (2019d), "Nonlinear vibration and modal analysis of FG nanocomposite sandwich beams reinforced by aggregated CNTs", *Polym. Eng. Sci.*, **59**(7), 1362-1370. doi: 10.1002/pen.25119.

Qin, Z., Yang, Z., Zu, J. and Chu, F. (2018), "Free vibration analysis of rotating cylindrical shells coupled with moderately thick annular plates", *Int. J. Mech. Sci.*, **142**–**143**, 127-139. doi: 10.1016/j.ijmecsci.2018.04.044.

Qin, Z., Safaei, B., Pang, X. and Chu, F. (2019), "Traveling wave analysis of rotating functionally graded graphene platelet reinforced nanocomposite cylindrical shells with general boundary conditions", *Results Phys.*, **15**, 102752. doi: 10.1016/j.rinp.2019.102752.

Qin, Z., Zhao, S., Pang, X., Safaei, B. and Chu, F. (2020), "A unified solution for vibration analysis of laminated functionally graded shallow shells reinforced by graphene with general boundary conditions", *Int. J. Mech. Sci.*, **170**, 105341. doi: https://doi.org/10.1016/j.ijmecsci.2019.105341.

Reddy, J.N. (2004), '*Mechanics of Laminated Composite Plates and Shells: Theory and Analysis*'.

Safaei, B., Naseradinmousavi, P. and Rahmani, A. (2016), "Development of an accurate molecular mechanics model for buckling behavior of multi-walled carbon nanotubes under axial compression", *J. Mol. Graph. Model.*, **65**, 43-60. doi: 10.1016/j.jmgm.2016.02.001.

Safaei, B., Moradi-Dastjerdi, R. and Chu, F. (2018a), "Effect of thermal gradient load on thermo-elastic vibrational behavior of sandwich plates reinforced by carbon nanotube agglomerations", *Compos. Struct.*, **192**, 28-37. doi: 10.1016/j.compstruct.2018.02.022.

Safaei, B., Fattahi, A.M. and Chu, F. (2018b), "Finite element study on elastic transition in platelet reinforced composites",

Microsyst. Technol., **24**(6), 2663-2671. doi: 10.1007/s00542-017-3651-y.
Safaei, B., Moradi-Dastjerdi, Rasool, Qin, Z. and Chu, F. (2019a), "Frequency-dependent forced vibration analysis of nanocomposite sandwich plate under thermo-mechanical loads", *Compos. Part B Eng.*, **161**, 44-54. doi: 10.1016/j.compositesb.2018.10.049.
Safaei, B., Khoda, F.H. and Fattahi, A.M. (2019b), "Non-classical plate model for single-layered graphene sheet for axial buckling", *Adv. Nano Res.*, **7**(4), 265-275. doi: 10.12989/anr.2019.7.4.265.
Safaei, B., Ahmed, N.A. and Fattahi, A.M. (2019c), "Free vibration analysis of polyethylene/CNT plates", *Eur. Phys. J. Plus*, **134**, 271. doi: 10.1140/epjp/i2019-12650-x.
Safaei, B., Moradi-Dastjerdi, Rasool, Qin, Z., Behdinan, K. and Chu, F. (2019d), "Determination of thermoelastic stress wave propagation in nanocomposite sandwich plates reinforced by clusters of carbon nanotubes", *J. Sandw. Struct. Mater.*, doi: 10.1177/109963621984828. doi: 10.1177/1099636219848282.
Safaei, B., Moradi-Dastjerdi, R., Behdinan, K. and Chu, F. (2019c) "Critical buckling temperature and force in porous sandwich plates with CNT-reinforced nanocomposite layers", *Aerosp. Sci. Technol.*, **91**, 175-185. doi: 10.1016/j.ast.2019.05.020.
Safaei, B., Moradi-Dastjerdi, R., Behdinan, K., Qin, Z. and Chu, F. (2019f), "Thermoelastic behavior of sandwich plates with porous polymeric core and CNT clusters/polymer nanocomposite layers", *Compos. Struct.*, **226**, 111209. doi: 10.1016/J.COMPSTRUCT.2019.111209.
Sahmani, S. and Safaei, B. (2020), "Influence of homogenization models on size-dependent nonlinear bending and postbuckling of bi-directional functionally graded micro/nano-beams", *Appl. Math. Model.*, **82**, 336-358. doi: 10.1016/j.apm.2020.01.051.
Sciamanna, V., Nait-Ali, B. and Gonon, M. (2015), "Mechanical properties and thermal conductivity of porous alumina ceramics obtained from particle stabilized foams", *Ceram. Int.*, **41**(2), 2599–2606. doi: 10.1016/j.ceramint.2014.10.011.
Sehoul, M., Benguediab, M., Bakora, A. and Tounsi, A. (2017), "Free vibrations of laminated composite plates using a novel four variable refined plate theory", *Steel Compos. Struct.*, **24**(5), 603-613. https://doi.org/10.12989/scs.2017.24.5.603.
Setoodeh, A.R., Malekzadeh, P. and Nikbin, K. (2009), "Low velocity impact analysis of laminated composite plates using a 3D elasticity based layerwise FEM", *Mater. Des.*, **30**(9), 3795-3801. doi: 10.1016/j.matdes.2009.01.031.
Setoodeh, A.R., Shojaee, M. and Malekzadeh, P. (2019), "Vibrational behavior of doubly curved smart sandwich shells with FG-CNTRC face sheets and FG porous core", *Compos. Part B Eng.*, **165**, 798-822. doi: 10.1016/J.COMPOSITESB.2019.01.022.
Sharma, N., Mahapatra, T.R., Panda, S.K. and Mehar, K. (2018) "Evaluation of vibroacoustic responses of laminated composite sandwich structure using higher-order finite-boundary element model", *Steel Compos. Struct.*, **28**(5), 629-639. doi: 10.12989/scs.2018.28.5.629.
Studart, A.R., Gonzenbach, U.T., Tervoort, E. and Gauckler, L.J. (2006), "Processing routes to macroporous ceramics: A review", *J. Am. Ceram. Soc.*, 1771-1789. doi: 10.1111/j.1551-2916.2006.01044.x.
Talebitooti, R., Daneshjoo, K. and Jafari, S.A.M. (2016), "Optimal control of laminated plate integrated with piezoelectric sensor and actuator considering TSDT and meshfree method", *Eur. J. Mech. A/Solids*, **55**, 199–211. doi: 10.1016/j.euromechsol.2015.09.004.
Thai, C.H., Ferreira, A.J.M., Carrera, E. and Nguyen-Xuan, H. (2013), "Isogeometric analysis of laminated composite and sandwich plates using a layerwise deformation theory", *Compos. Struct.*, **104**, 196-214. doi: 10.1016/J.COMPSTRUCT.2013.04.002.
Thai, H. and Choi, D. (2011), "A refined plate theory for functionally graded plates resting on elastic foundation", *Compos. Sci. Technol.*, **71**(16), 1850-1858. doi: 10.1016/j.compscitech.2011.08.016.
Tornabene, F., Fantuzzi, N., Bacciocchi, M. and Reddy, J.N. (2017), "A posteriori stress and strain recovery procedure for the static analysis of laminated shells resting on nonlinear elastic foundation", *Compos. Part B Eng.*, **126**, 162-191. doi: 10.1016/J.COMPOSITESB.2017.06.012.
Tornabene, F., Viola, E. and Fantuzzi, N. (2013), "General higher-order equivalent single layer theory for free vibrations of doubly-curved laminated composite shells and panels", *Compos. Struct.*, **104**, 94-117.
Vinson, J.R. (2001), "Sandwich Structures", *Appl. Mech. Rev.*, **54**(3), 201. doi: 10.1115/1.3097295.
Wang, Y.Q. (2014), "Nonlinear vibration of a rotating laminated composite circular cylindrical shell: Traveling wave vibration", *Nonlinear Dyn.*, **77**(4), 1693-1707. doi: 10.1007/s11071-014-1410-5.
Wang, Z., Yu, T., Bui, T.Q., Trinh, N.A., Luong, N.T.H., Duc, N.D. and Doan, D.H. (2016), "Numerical modeling of 3-D inclusions and voids by a novel adaptive XFEM", *Adv. Eng. Softw.*, **102**, 105-122. doi: 10.1016/j.advengsoft.2016.09.007.
Wu, X., Lu, C., Xu, H., Zhang, X. and Zhou, Z. (2014), "Biotemplate synthesis of polyaniline@cellulose nanowhiskers/natural rubber nanocomposites with 3D hierarchical multiscale structure and improved electrical conductivity", *ACS Appl. Mater. Interfaces*, **6**(23), 21078–21085. doi: 10.1021/am505924z.
Xiaohui, R., Zhen, W. and Bin, J. (2018), "A refined sinusoidal theory for laminated composite and sandwich plates", *Mech. Adv. Mater. Struct.* doi: 10.1080/15376494.2018.1538469.
Xie, B., Sahmani, S., Safaei, B. and Xu, B. (2020) "Nonlinear secondary resonance of FG porous silicon nanobeams under periodic hard excitations based on surface elasticity theory", *Eng. Comput.*, doi: 10.1007/s00366-019-00931-w.
Xu, K., Yuan, Y. and Li, M. (2019), "Buckling behavior of functionally graded porous plates integrated with laminated composite faces sheets", *Steel Compos. Struct.*, **32**(5), 633-642. https://doi.org/10.12989/scs.2019.32.5.633.
Xue, Y., Jin, G., Ma, X., Chen, H., Ye, T., Chen, M. and Zhang, Y. (2019), "Free vibration analysis of porous plates with porosity distributions in the thickness and in-plane directions using isogeometric approach", *Int. J. Mech. Sci.*, **152**, 346-362. doi: 10.1016/j.ijmecsci.2019.01.004.
Yan, D.X., Ren, P.G., Pang, H., Fu, Q., Yang, M.B. and Li, Z.M. (2012) "Efficient electromagnetic interference shielding of lightweight graphene/polystyrene composite", *J. Mater. Chem.*, **22**(36), 18772-18774. doi: 10.1039/c2jm32692b.
Yang, J., Chen, D. and Kitipornchai, S. (2018), "Buckling and free vibration analyses of functionally graded graphene reinforced porous nanocomposite plates based on Chebyshev-Ritz method", *Compos. Struct.*, **193**, 281-294. doi: 10.1016/J.COMPSTRUCT.2018.03.090.
Yang, X., Sahmani, S. and Safaei, B. (2020), "Postbuckling analysis of hydrostatic pressurized FGM microsized shells including strain gradient and stress-driven nonlocal effects", *Eng. Comput.*, doi: 10.1007/s00366-019-00901-2.
Yi, H., Sahmani, S. and Safaei, B. (2020), "On size-dependent large-amplitude free oscillations of FGPM nanoshells incorporating vibrational mode interactions", *Arch. Civ. Mech. Eng.*, **20**(2), 48. doi: 10.1007/s43452-020-00047-9.
Yu, T., Yin, S., Bui, T.Q., Xia, S., Tanaka, S. and Hirose, S. (2016), "NURBS-based isogeometric analysis of buckling and free vibration problems for laminated composites plates with complicated cutouts using a new simple FSDT theory and level

set method'', *Thin Wall. Struct.*, **101**, 141-156. doi: 10.1016/j.tws.2015.12.008.

Yuan, Y., Zhao, K., Sahmani, S. and Safaei, B. (2020), ''Size-dependent shear buckling response of FGM skew nanoplates modeled via different homogenization schemes'', *Appl. Math. Mech.*, 1-18. doi: 10.1007/s10483-020-2600-6.

Zargar, O., Mollaghaee-Roozbahani, M., Bashirpour, M. and Baghani, M. (2019), ''The application of Homotopy Analysis Method to determine the thermal response of convective-radiative porous fins with temperature-dependent properties'', *Int. J. Appl. Mech.*, doi: 10.1142/s1758825119500881.

Zargar, O., Masoumi, A. and Moghaddam, A.O. (2017), ''Investigation and optimization for the dynamical behaviour of the vehicle structure'', *Int. J. Automot. Mech. Eng.*, **14**, 4196-4210. doi: 10.15282/ijame.14.2.2017.7.0336.

Zhang H., *et al*. (2020), ''Study on vibro-acoustic property of composite laminated rotary plate-cavity system based on a simplified plate theory and experimental method'',. *Int. J. Mech. Sci.*, **167**, 105264. DOI: 10.1016/j.ijmecsci.2019.105264.

Zhao, J., Xie, F., Wang, A., Shuai, C., Tang, J. and Wang, Q. (2019a), ''Dynamics analysis of functionally graded porous (FGP) circular , annular and sector plates with general elastic restraints'', *Compos. Part B*, **159**, 20-43. doi: 10.1016/j.compositesb.2018.08.114.

Zhao, J., Xie, F., Wang, A., Shuai, C., Tang, J. and Wang, Q. (2019b), ''Vibration behavior of the functionally graded porous (FGP) doubly-curved panels and shells of revolution by using a semi-analytical method'', *Compos. Part B*, **157**, 219-238. doi: 10.1016/j.compositesb.2018.08.087.

CC